IMPACT-CAUSED REGOLITH REWORKING WITHIN THE POLAR REGIONS OF THE MOON: MECHANICAL AND GEOCHEMICAL ASPECTS. A. T. Basilevsky[1], M. A. Kreslavsky[2], V. A. Dorofeeva[1], Yuan Li[3] and LiGang Fang[3], [1]Vernadsky Institute of Geochemistry and Analytical Chemistry RAS, Kosygin str., 19, 119991, Moscow, Russia, atbas@geokhi.ru, [2]University of California – Santa Cruz, Santa Cruz, CA, 95064 USA, mkreslav@ucsc.edu, [3]Suzhou vocational University, SuZhou, 21509, China, lysongly@sina.com.

Introduction: Regolith in polar areas of the Moon contains water ice and other frozen volatiles [e.g., 1-3] and thus is a subject of interest both for fundamental lunar science and for practical needs. One of the topics interesting both for fundamental and practical issues is evolution of the ice-bearing deposits with time [e.g., 4,5]. In this work we consider part of this topic, namely, question of impact-caused reworking of polar regolith and its effect on water ice and other ices in it. Cratering rate in lunar polar areas of the Moon comparing to that in the lower latitudes is smaller only by ~20% [6] so for this work it is considered the same as for all lunar surface. The question of impact-caused reworking of lunar regolith was considered long time ago [e.g., 7-9] and it looks that those early considerations are still valid. Recently this issue was revisited with more sophisticated models [e.g., 10,11] and applied them to analysis of water ice in the lunar polar areas [e.g., 12-14]. In this work we use simple analytical approach of [9] to the issue of polar regolith by considering characteristics of population of small (D <1-2 km) lunar craters.

Our Approach:

We present simple estimates of regolith reworking by small impacts following [9]. The population of small craters can be divided into two parts: equilibrium and non-equilibrium sub-populations with boundary between them at the “critical” crater diameter D_{cr} (Fig. 1).

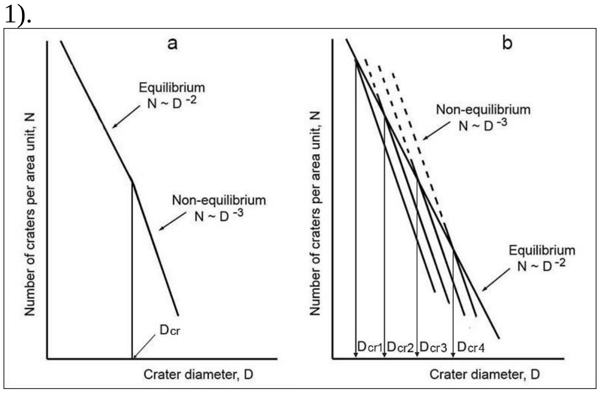

Fig.1. a) Schematic plot of number of craters (N) with diameter greater than D per unit area as a function of D; logarithmic scale on both axes; D_{cr} is a boundary diameter between the equilibrium and non-equilibrium subpopulations; b) The same plot showing increase of D_{cr} with time.

Random character of spatial distribution of craters leads to variations of the reworking depth from place to place. They are presented as minimum, median and maximum regolith thicknesses: 1) Minimum thickness H_{min} is in the place where the reworking was on minimal depth; calculated from [9] for the case $n = 1$. 2) Median thickness H_{med} represents the 50% frequency in the thickness distribution in the area. 3) Maximum thickness H_{max} is the depth of the largest completely eroded crater in the given area, that is depth of the crater with diameter equal D_{cr}. It can be shown that:

$$H_{min} = D_{cr}/50, H_{med} = D_{cr}/25, H_{max} = D_{cr}/5.$$

We compared our shown below results with model used by [11] and found similarity of our and their results.

Calculation Results:

Below are presented the minimum, median and maximum thickness of regolith on the floors of craters Shoemaker (D = 52 km, T = 4.16 Ga), Sverdrup (D = 33 km, T = 3.8 Ga), and Shackleton (D = 21 km, T = 3.15 Ga), all close to South pole, and for comparison show estimates for the Luna-16, 17 and 24 landing sites. Also, for these areas we calculated numbers (n) of the reworking acts down to the depths 2, 1.5, 1, 0.5, 0.2 and 0.05 m as well as average numbers (n_{av}) of the reworking acts down to these depths (see Table).

Parameter	L24	L16, 17	Shac	Sver	Shoe
D_{cr}, *m*	80	100	~80	~350	~1000
Cratering intensity*	2,5	6	2,5	200	1000
H_{min}, *m*	1,6	2	1,6	7	20
H_{med}, *m*	3,2	4	3,2	14	40
H_{max}, *m*	16	20	16	70	200
n H = 2 *m*	1,6	2	1,6	7	20
n_{av} H = 2 *m*	16	20	16	69	198
n H = 1,5 *m*	~2	~3	~2	9	27
n_{av} H = 1,5 *m*	19	29	19	87	260
n H = 1 *m*	~3	4	~3	14	40
n_{av} H = 1 *m*	28	37	28	129	368
n H = 0,5 *m*	6	8	6	28	80
n_{av} H = 0,5 *m*	51	68	51	238	681
n H = 0,2 *m*	16	20	16	70	200
n_{av} H = 0,2 *m*	121	150	121	531	1518
n H = 0,05 *m*	64	80	64	280	800
n_{av} H = 0,05*m*	397	500	397	1739	4968

**Cratering intensity in Eratosthenian-Copernican periods is assumed = 1.*

It is seen from the Table that calculated by us H_{med} in the Luna-16, 17, 24 sites is between 3.2 and 4 m, that agrees with estimations based on the Arecibo radar data [15]. H_{med} on the floor of relatively young (3.15 Ga) crater Shackleton is 3.2 m that looks reasonable. H_{med} on the floor of the older crater Sverdrup (3.8 Ga) is 14 m, that agrees with the results of [15] – their Fig. 11. These agreements suggest that our approach to estimate thickness of lunar regolith is valid and consider as acceptable our estimate of the 40 m H_{med} on the floor of the oldest among the considered crater Shoemaker (4.16 Ga).

Discussion and conclusions:

Regolith in polar areas of the Moon accumulated and reworked like in other lunar areas excavating the lower layers and burying the upper ones. Estimated contents of H_2O ice in it (<0,0n to n mass. % [1-3, 16]), probably do not influence significantly on this process. In this process at each given impact some portion of the regolith material is compressed. If compression is low that is typical at relatively large distances from the impact point, it should lead to moderate heating with melting and vaporization of the H_2O ice and other ices. Closer to the impact point the heating is much higher. Impactors bombarding lunar surface have velocities from ~2,5 to ~70 km/s [6,17,18] that should lead to very high heating especially if target is porous. The earth-based observations led to finding on the Moon 112 light flashes that allowed to estimate sizes of the impactors (cm-dm) and brightness temperatures of those flashes (1000 to 7000 K with average ~2700 K [19]).

Impact heating of polar regolith should lead to vaporization and partial decomposition of at least part of the frozen volatiles and silicate-oxide-sulfide minerals providing possibilities for escape of part of volatiles to the open space with their physico-chemical differentiation and for chemical reactions between all the components leading, for example, to oxidation of Fe^0 and Fe^{2+} to Fe^{3+}. This effect was recently discovered by [20] who analyzing the M^3 data found presence of hematite at the high northern and southern latitudes of the Moon (Fig. 2) probably caused by reactions with involvement of the polar H_2O measured by LEND [21] (Fig. 3). Comparison of Figs 2 and 3 shows that spatial distribution of hematite correlates better with distribution of H_20 measured by LEND than with that measured by the M^3 instrument suggesting that the hematite formation is within the dm-m thick layer.

Acknowledgments: ATB was supported by the RSF grant № 21-17-00035: Estimates of the rate of exogenous resurfacing on the Moon. Yuan Li was supported by the JiangSu Grant 20KJD160001. Authors are grateful to A.B. Sanin, C. Pieters, B.A. Ivanov, O.I. Yakovlev, M.V. Gerasimov, and Tiantian Liu for their help.

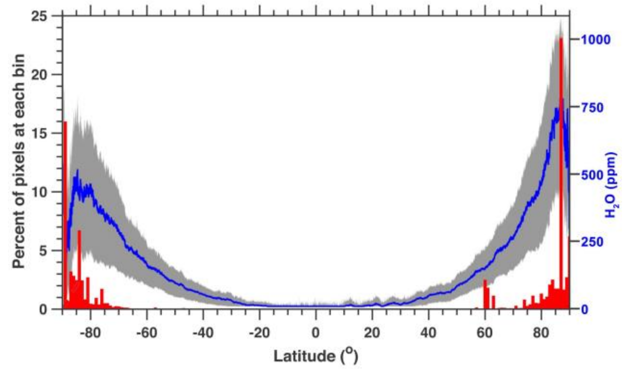

Fig.2. Red – detections of hematite binned at 1 latitude degree, Blue – water content mapped from the M^3 data; modified from Fig. S2 of [20].

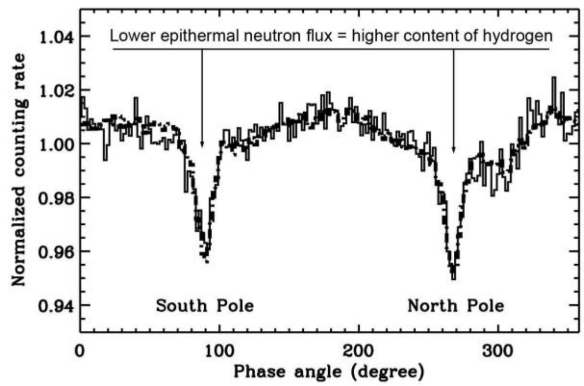

Fig.3. Latitude variations of epithermal neutron flux across the lunar surface measured by LEND; modified from Fig. 12 in [21].

References: [1] Feldman W. C. (1998) *Science, 281*, 1496-1500. [2] Mitrofanov I. G., et al (2010) *Science, 330*, 483-486. [3] Colaprete A. (2010) *Science, 330*, 463-468. [4] Li S. et al. (2018) PNAS, *115(36).* 8907–8912. [5] Farrell W. M. et al. (2019) *GRL, 46*, 8680–8688. [6] Le Feuvre M., Wieczorek M. A. (2008) *Icarus, 197*, 291–306. [7] Shoemaker E. M. et al. (1969) *JGR, 74(25)*, 6081–6119. [8] Gault D. et al. (1974) *Proc. 5th Lunar Conf.*, 2365–2386. [9] Basilevsky A.T. (1974) *Kosmicheskie Issledovaniya, XII, Is. 4,* 606-609 (in Russian). [10] Costello E.S. et al. (2018) *Icarus., 314.* 327–344. [11] Hirabayashi M. et al. (2018) *JGR Planets, 123*, 527–543. [12] Hurley D.M. et al. (2012) *GRL, 39,* L09203. 13] Cannon K. M. and Britt D. T. (2020) *Icarus, 347*, 113778. [14] Costello E. S. (2020) *JGR Planets, 125(3),* e06172. [15] Shkuratov Y., Bondarenko N. (2001) *Icarus, 149(2),* 329–338. [16] Sanin A.B. et al. (2017) *Icarus, 283*, 20–30. [17] Melosh H.J. (2011) *Planetary Surface Processes*. Camb. Univ. Press. 500 p. [18] Werner S.C., Ivanov B.A. (2015) *Treatise on Geophysics*. 327-365. [19] Avdellidou C.et al. (2021) *Pl. Space Sci. 200.* 105201. [20] Li S. (2020) *Science Advances, 6*, eaba 1940. [21] Litvak M. L. et al (2012) *JGR, 117,* E00H22.